

A thermodynamic model for the simultaneous charge/spin order transition in $\text{LaCu}_3\text{Fe}_4\text{O}_{12}$

This article has been downloaded from IOPscience. Please scroll down to see the full text article.

2012 J. Phys.: Condens. Matter 24 495601

(<http://iopscience.iop.org/0953-8984/24/49/495601>)

View [the table of contents for this issue](#), or go to the [journal homepage](#) for more

Download details:

IP Address: 200.0.233.52

The article was downloaded on 23/04/2013 at 21:20

Please note that [terms and conditions apply](#).

A thermodynamic model for the simultaneous charge/spin order transition in $\text{LaCu}_3\text{Fe}_4\text{O}_{12}$

R Allub and B Alascio

Centro Atómico Bariloche, (8400) S C de Bariloche, Argentina

E-mail: allub@cab.cnea.gov.ar

Received 1 July 2012, in final form 27 October 2012

Published 16 November 2012

Online at stacks.iop.org/JPhysCM/24/495601

Abstract

$\text{LaCu}_3\text{Fe}_4\text{O}_{12}$ undergoes a phase transition at 393 K from an antiferromagnetic insulating state at low temperatures to a paramagnetic metallic state above the critical temperature. We build a basic model for the electronic structure of this material that allows us to extract the mechanism that governs the transition and calculate the stability of the different phases. It also allows us to speculate on the effect of pressure on this material to build a T - p phase diagram.

1. Introduction

The transition-metal oxides (ABO_3) forming perovskite-like structures have been the subject of much experimental and theoretical research due to the large variety of physical properties found in them [1–3]. The motivation for research is not only based on academic interest but also on the possible technological applications. Colossal magnetoresistance, giant dielectric constant, ferrimagnetism, ferroelectricity and other peculiar properties are intertwined in the material and can be modified by the effect of temperature, pressure, chemical composition or external fields [4, 5]. In general, changes in the physical properties are a consequence of valence changes of the transition-metal elements forming the compound. The B element is usually dominant in the physical behavior of the material and its valence is modified by partially substituting the three-valent rare earth element by a two-valent alkaline earth. This substitution often results in a transition from an insulating to a half-metallic magnetoresistant material [6].

Recently Long *et al* [7] have reported an unusual temperature induced valence change in the double ordered perovskite $\text{LaCu}_3\text{Fe}_4\text{O}_{12}$. When heated from low temperatures, the compound shows a first-order transition from an antiferromagnetic insulator to a paramagnetic metal at 393 K. They show that the phase transition occurs as a consequence of the transfer of one hole per Cu to Fe, so the transition is from $\text{LaCu}_3^+\text{Fe}_4^{3+}\text{O}_{12}$ to $\text{LaCu}_3^+\text{Fe}_4^{3.75+}\text{O}_{12}$. Changhoon Lee *et al* [8] studied the effect of magnetic interactions Fe–Fe and Fe–Cu on the transition on the basis of density functional analysis.

Since at the transition the physical properties of the material change abruptly and substantially, it would be desirable to be able to control temperature, pressure and possible doping of this perovskite at the point at which the transition takes place. To do this it is necessary to have an idea of the mechanism leading to the phase transition. The aim of this paper is to give a simple description of the transition, suggest a pressure–temperature (T - p) phase diagram for this compound, and describe the properties of the different phases.

To this end we resort to a Falikov–Kimball (FK) model [9]. The FK model includes both extended conduction electrons and strongly correlated localized electrons with the insulator–metal transition occurring when the localized electrons (or holes) move into the conduction bands.

According to Long *et al*'s charge transfer results, we take two competing electronic configurations around the critical temperature (T_N). In order to reduce the system to an FK model we consider: (i) below T_N we have the Cu^{3+} ion containing six electrons in the 3d t_{2g} orbitals and two electrons in the 3d e_g orbitals, forming a nonmagnetic state, while Fe^{3+} , containing five electrons in the 3d t_{2g} orbitals, forms a $S = 5/2$ spin state; (ii) above T_N , we have the Cu^{2+} ion containing six electrons in the 3d t_{2g} orbitals and three electrons in the 3d e_g orbitals, forming a $S = 1/2$ state, while the $\text{Fe}^{3.75+}$ result from four localized electrons forming a $S = 2$ spin state in the 3d t_{2g} orbitals and a 0.25 itinerant electron. It is the Coulomb repulsions between the added electron in Cu and the itinerant electrons in Fe that give rise to the FK model. Figure 1 shows the two competing electronic configurations

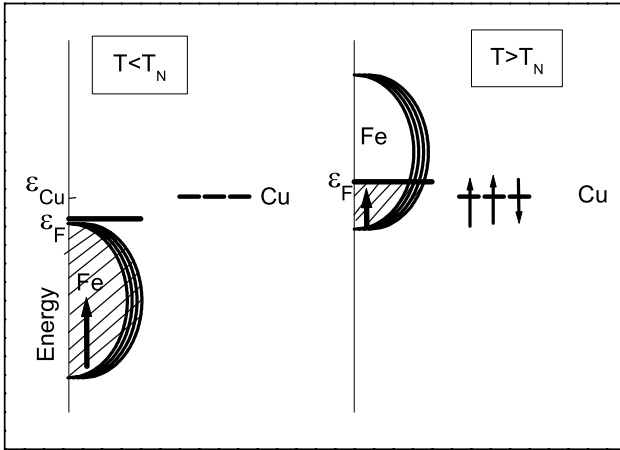


Figure 1. Schematic sketch of the relevant electronic structure in the AF and PM phases (spin up). Figure shows the density of states per formula unit: four Fe bands and three localized Cu levels between which electron transfer takes place. For $T < T_N$, we can see the Fermi level (ε_F) just above the four degenerate Fe filled bands and below the three degenerate Cu levels (empty). For $T > T_N$, the figure shows the ε_F inside the four Fe bands and just above the three single occupied Cu levels. The arrow inside the bands shows the localized spin of Fe.

around T_N in a simplified scheme. We draw the density of states per formula unit with three Cu atoms and four Fe. For $T < T_N$ (the insulating room temperature phase), the figure shows the Cu levels empty and Fe bands filled. In contrast, for $T > T_N$ (the high temperature metallic phase), we can see the three Cu levels filled and the four Fe bands partially filled.

We assume the exchange coupling between e_{2g} and t_{2g} in each Fe site is strong enough to consider the spin of the mobile electrons in each site always to be aligned with the localized electrons in that site. This condition leads to a half-metallic band in which the hopping is conditioned by the spin correlation between nearest-neighbor Fe sites [10].

In the following section we set up the model free energy as a function of the Cu occupation and the magnetization of the Fe ions in the ferromagnetic or antiferromagnetic phases.

In section 3 we minimize the free energy to obtain the stable state at each temperature and discuss the results. Section 4 consists of the conclusions.

2. Model

We propose a model which contains the following basic ingredients.

(a) A band of extended states, which we assume originates from the iron 3d states hybridized with the oxygen atoms lying in between. Due to strong Hund's coupling on Fe sites, itinerant electrons with spin σ can hop only to Fe sites with *parallel* localized spins. These extended states give the kinetic energy E_K and this favors the ferromagnetic order of the localized Fe spins. Beside this energy, to determine the magnetic behavior of the system, we also consider the antiferromagnetic superexchange interaction energy E_M between the Fe localized spins, which favors the antiferromagnetic order of Fe spins.

(b) A set of more localized states (assumed to originate in Cu atoms), with energy E_L .

(c) Finally, we have the FK contribution E_{FK} , which arises from the Coulomb repulsion between particles in localized and extended states, which is treated in the mean-field approximation.

With these ingredients, the charge transfer occurs due to the superposition of the extended and localized states, which results from two main effects: the effective difference in energies between them, which depends on the charge at each type of state on one side (the mean-field Coulomb repulsion favors electrons to occupy either of the states) and the width of the band states on the other (see figure 1). Since we assume double-exchange [11] to act as the mechanism that allows the formation of extended states, the spin order is basic in determining the bandwidth. Spin ordering determines not only the bandwidth but it is also the main source of entropy, which drives the transition from ordered to disordered states.

Both, the entropy and the bandwidth are expressed in terms of magnetization of the iron states and we restrict our approach to simple magnetic structures: ferromagnetic, paramagnetic, and antiferromagnetic phases.

In order to write the model free energy per formula unit of the system, first we obtain the corresponding internal energy E . For this purpose, we need to calculate E_K , E_M , E_L , and E_{FK} .

2.1. The kinetic energy

In the mean-field approximation for the FK term, the only nontrivial energy is the kinetic energy of the itinerant electrons E_K which becomes somewhat complicated due to the need to take into account the strong correlation between Fe orbitals. To take this into account we resort to a simple technique that we have often used before [12–14] based on a mean-field approximation on the hopping term which is described below. To obtain a first approximation to this energy, we consider first a single-band model Hamiltonian:

$$H_{Fe} = \varepsilon_{Fe} \sum_{i,\sigma} c_{i\sigma}^\dagger c_{i\sigma} - \sum_{\langle i,j \rangle, \sigma} t_{\mu_i, \mu_j, \sigma} c_{i\sigma}^\dagger c_{j\sigma}, \quad (1)$$

where ε_{Fe} is the Fe site diagonal energy, $c_{i\sigma}^\dagger$, $c_{i\sigma}$ creates and destroys, respectively, an itinerant electron with spin σ (\uparrow , \downarrow) at Fe site i , μ_i ($+$, $-$) refers to the localized spin of Fe at site i (Ising model), and $t_{\mu_i, \mu_j, \sigma}$ is the nearest-neighbor hopping term t_{Fe} when σ , μ_i , and μ_j are all parallel and zero in any other case. This hopping term favors a ferromagnetic background of the localized Fe spins [10]. In order to obtain the density of states for itinerant electrons, we calculate local Green's functions in an interpenetrating Bethe lattice using the renormalized perturbation expansion (RPE) [15]. The RPE connects the propagator at site i to propagators at the nearest-neighbor sites $i + \delta$ which exclude visiting site i again and which we will denote by small g s. These new propagators are in turn connected to propagators of the same type at sites $i + \delta + \delta'$, etc, so that the Green's function at each site depends, through this chain, on the local spin

configurations of the Fe. This procedure leads to different Green's functions for different sites, according to the local spin configurations around the site. We are interested in the configurational average of Green's functions over all possible spin configurations. This configurational average over local spin directions is assumed to be the same at every site of the same sublattice, to restore translational invariance in the spirit of the mean-field theories as ATA, CPA, etc. To this end we consider two interpenetrating sublattices α and β , characterized by the magnetization m_α and m_β , respectively, and we introduce $G_{\sigma\mu}^\alpha$ ($G_{\sigma\mu}^\beta$) which include the probabilities $v_\pm^\alpha = (1 \pm m_\alpha)/2$ (v_\pm^β) that an α (β) Fe ion has for its localized spin \uparrow (\downarrow). In accordance with the model Hamiltonian, we have $G_{\uparrow-}^\alpha = G_{\downarrow+}^\alpha = G_{\uparrow-}^\beta = G_{\downarrow+}^\beta = 0$ and only $G_{\uparrow+}^\alpha$ and $G_{\uparrow+}^\beta$ (or $G_{\downarrow-}^\alpha$ and $G_{\downarrow-}^\beta$) are given by

$$G_{\uparrow+}^\alpha = \frac{v_+^\alpha}{[\omega - \varepsilon_{\text{Fe}} - z t_{\text{Fe}}^2 g_{\uparrow+}^\beta]}, \quad (2)$$

where we assume that the sum over neighbors can be replaced by the number of nearest neighbors z times their average Green functions $g_{\uparrow+}^\beta$ given by

$$g_{\uparrow+}^\beta = \frac{v_+^\beta}{[\omega - \varepsilon_{\text{Fe}} - (z-1)t_{\text{Fe}}^2 g_{\uparrow+}^\alpha]}, \quad (3)$$

with

$$g_{\uparrow+}^\alpha = \frac{v_+^\alpha}{[\omega - \varepsilon_{\text{Fe}} - (z-1)t_{\text{Fe}}^2 g_{\uparrow+}^\beta]}. \quad (4)$$

Similarly, we can write

$$G_{\uparrow+}^\beta = \frac{v_+^\beta}{[\omega - \varepsilon_{\text{Fe}} - z t_{\text{Fe}}^2 g_{\uparrow+}^\alpha]}. \quad (5)$$

The Green's functions for down electrons are obtained by replacing \uparrow by \downarrow and $+$ by $-$.

Let us mention that, when the coordination number $z \rightarrow \infty$, the functions $g \rightarrow G$ and the above equations reduce to those used in a dynamical mean-field approach. In that case $z t_{\text{Fe}}^2$ scales as $W_{\text{Fe}}^2/4$, being half the bandwidth. So that the Green's functions reduce to

$$G_{\uparrow+}^\alpha = \frac{v_+^\alpha}{[\omega - \varepsilon_{\text{Fe}} - t'^2 G_{\uparrow+}^\beta]} \quad (6)$$

and

$$G_{\uparrow+}^\beta = \frac{v_+^\beta}{[\omega - \varepsilon_{\text{Fe}} - t'^2 G_{\uparrow+}^\alpha]}, \quad (7)$$

with $t'^2 = W_{\text{Fe}}^2/4$.

In this work, we consider only three possible magnetic phases for Fe: ferromagnetic (F), antiferromagnetic (AF), and paramagnetic (P).

In the F phase we have $m_\alpha = m_\beta = m$ (the average site magnetization), so that $G_{\uparrow+}^\alpha = G_{\uparrow+}^\beta$ and we obtain from

equations (6) and (7):

$$G_{\uparrow+}^\alpha = \frac{\omega \pm \sqrt{\omega^2 - 4v_+ t'^2}}{2t'^2}, \quad (8)$$

where we take $\varepsilon_{\text{Fe}} = 0$ and $v_+ = (1 + m)/2$. The corresponding density of states per Fe site can be written as $\rho_{\uparrow+}(m, \omega) = (-1/\pi)\text{Im}G_{\uparrow+}^\alpha = \sqrt{4v_+ t'^2 - \omega^2}/2\pi t'^2$. Therefore, $n_{\uparrow+} = \int_{-\infty}^{\varepsilon_{\text{F}}} \rho_{\uparrow+}(m, \omega) d\omega$ is given by

$$n_{\uparrow+} = \frac{v_+}{2} + \frac{\varepsilon_{\text{F}} \sqrt{4v_+ t'^2 - \varepsilon_{\text{F}}^2}}{4\pi t'^2} + \frac{v_+}{\pi} \sin^{-1} \left(\frac{\varepsilon_{\text{F}}}{2t' \sqrt{v_+}} \right), \quad (9)$$

where ε_{F} is the Fermi energy. The corresponding kinetic energy is $E_{\uparrow+} = \int_{-\infty}^{\varepsilon_{\text{F}}} \omega \rho_{\uparrow+}(m, \omega) d\omega$ and this gives

$$E_{\uparrow+} = - \frac{\left(\sqrt{4v_+ t'^2 - \varepsilon_{\text{F}}^2} \right)^3}{6\pi t'^2}. \quad (10)$$

In a similar manner, for down electrons, we can write $\rho_{\downarrow-}(m, \omega) = (-1/\pi)\text{Im}G_{\downarrow-}^\alpha = \sqrt{4v_- t'^2 - \omega^2}/2\pi t'^2$, with $v_- = (1 - m)/2$.

Then $n_{\downarrow-}$ and $E_{\downarrow-}$ are obtained by replacing v_+ by v_- in equations (9) and (10). Taking into account these results, we obtain the average number of electrons per site of Fe in the ferromagnetic phase as $n_{\text{Fe}}(m, \varepsilon_{\text{F}}) = n_{\uparrow+} + n_{\downarrow-}$ and the kinetic energy as $E_{\text{band}}(m, \varepsilon_{\text{F}}) = E_{\text{bandF}}(m, \varepsilon_{\text{F}}) = E_{\uparrow+} + E_{\downarrow-}$.

In the AF phase we have $m_\alpha = -m_\beta = m$ and solving equations (6) and (7) we obtain

$$G_{\uparrow+}^\alpha = \frac{(\omega^2 + t'^2 m)}{2v_+ t'^2 \omega} \pm \frac{\sqrt{\omega^4 + t'^4 m^2 - 2t'^2 \omega^2}}{2v_+ t'^2 |\omega|} \quad (11)$$

and

$$G_{\uparrow+}^\beta = \frac{(\omega^2 - t'^2 m)}{2v_- t'^2 \omega} \pm \frac{\sqrt{\omega^4 + t'^4 m^2 - 2t'^2 \omega^2}}{2v_- t'^2 |\omega|}. \quad (12)$$

It is easy to see that $G_{\downarrow-}^\beta = G_{\uparrow+}^\alpha$ and $G_{\downarrow-}^\alpha = G_{\uparrow+}^\beta$. So that the corresponding AF density of states per

site is $\rho_{\uparrow+}(m, \omega) = \sqrt{2t'^2 \omega^2 - (\omega^4 + t'^4 m^2)}/(2\pi t'^2 |\omega|)$ and the same for $\rho_{\downarrow-}(m, \omega)$. From here we can obtain the total average number of particles per AF site as $n_{\text{Fe}}(m, \varepsilon_{\text{F}}) = 2 \int_{-\infty}^{\varepsilon_{\text{F}}} \rho_{\uparrow+}(m, \omega) d\omega$ and the corresponding kinetic energy $E_{\text{band}}(m, \varepsilon_{\text{F}}) = E_{\text{bandAF}}(m, \varepsilon_{\text{F}}) = 2 \int_{-\infty}^{\varepsilon_{\text{F}}} \omega \rho_{\uparrow+}(m, \omega) d\omega$.

For $m = 0$ ($m_\alpha = m_\beta = 0$), our previous results (for F or AF) reduce to the kinetic energy ($E_{\text{bandP}}(\varepsilon_{\text{F}})$) in the paramagnetic phase.

2.2. The free energy

Considering three Cu atoms and four Fe atoms per formula unit, we can write the contribution of the local energy and the kinetic energy as $E_{\text{L}} + E_{\text{K}} = 3\varepsilon_{\text{Cu}} n_{\text{Cu}} + 4E_{\text{band}}(m, n_{\text{Fe}})$, where ε_{Cu} is the Cu site diagonal energy. Finally, charge conservation implies $3n_{\text{Cu}} + 4n_{\text{Fe}} = 4$. We consider now the

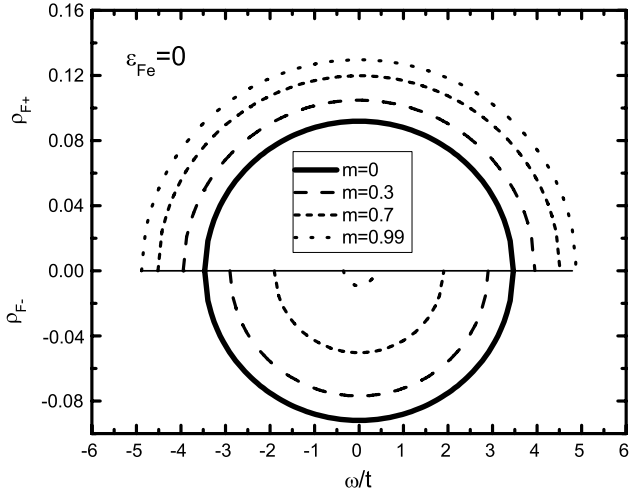


Figure 2. Paramagnetic ($m = 0$) and ferromagnetic density of states for spin \uparrow (ρ_{F+}) and \downarrow (ρ_{F-}) versus ω/t , for different values of the magnetization m and $\varepsilon_{Fe} = 0$. For $m = 1$, $\rho_{F-} = 0$.

magnetic energy contribution due to the number of localized electrons in t_{2g} Fe orbitals. In the F phase we take this energy as $E_{M,F} = K_0 m^2$, where $K_0 (>0)$ is an antiferromagnetic coupling constant. For the AF phase, as a first approximation, we consider $E_{M,AF} = -K_0(1 - \alpha n_{Cu})m^2$, where we take the coupling as a linear function of n_{Cu} . We introduce this factor to take into account a weakening of K_0 due to spin frustration produced by the antiferromagnetic coupling between the localized spin Cu electron and the Fe spins in nearest-neighbor sites. We fix the constant $\alpha = 0.3$ in order to fit the experimental data [7] at the transition: the extrapolated Néel temperature ($T_N^* \sim 600$ K) and the magnetization $m = m_\alpha = -m_\beta$. In this work, in order to introduce the model with a minimum number of parameters, we do not include an antiferromagnetic coupling between the localized Cu and Fe spins, which is small as compared to other parameters due to the fact that there is no direct connection between them.

Finally, we include an FK term, which is the term producing the first-order transition: $E_{FK} = 3Gn_{Cu}n_{Fe}$.

To proceed further, we need an expression for the difference in entropy between the considered phases. We assume three main contributions to this quantity: one magnetic dominant, due to the Fe spin, for which we take a numerical approximation to the Brillouin entropy for $S = 2$ as a function of magnetization, $S_{Fe} = \ln(5)(1 - m^2)^{2/3}$, the second and third are due to Cu levels and they are the configurational entropy of the Cu level occupation, $S_{Cu} = -[n_{Cu} \ln(n_{Cu}) + (1 - n_{Cu}) \ln(1 - n_{Cu})]$, and the magnetic entropy of the local spin, $S'_{Cu} = n_{Cu} \ln(2)$.

From the above considerations, we obtain the free energy as a function of the occupation numbers of the Cu orbitals (n_{Fe} is related to n_{Cu} by charge conservation) and the magnetization. Depending on the magnetic order, we can write three different expressions for the free energy by formula unit. The antiferromagnetic free energy takes the form

$$F_{AF} = 3\varepsilon_{Cu}n_{Cu} + 4E_{bandAF}(m, n_{Fe}) + E_{M,AF} + E_{FK} - 4TS_{Fe} - 3T(S_{Cu} + S'_{Cu}), \quad (13)$$

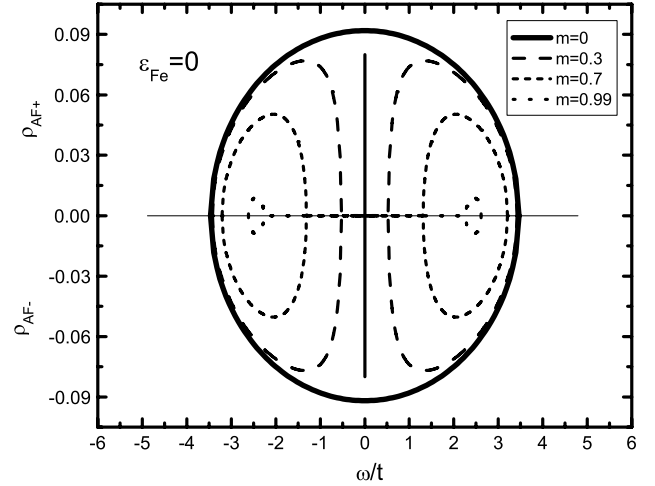


Figure 3. Antiferromagnetic density of states for spin \uparrow (ρ_{AF+}) and \downarrow (ρ_{AF-}) versus ω/t , for different values of the magnetization m and $\varepsilon_{Fe} = 0$. When m increases, the gap around $\omega = 0$ increases and $\rho_{AF\pm}$ decreases. For $m = 1$, $\rho_{AF\pm}$ disappears. The vertical full line at $\omega = 0$ represents the δ -peaks.

the ferromagnetic free energy is given by

$$F_F = 3\varepsilon_{Cu}n_{Cu} + 4E_{bandF}(m, n_{Fe}) + E_{M,F} + E_{FK} - 4TS_{Fe} - 3TS_{Cu}, \quad (14)$$

where we ignore the contribution of S'_{Cu} , due to the order of Cu spins in the F phase. Finally, the paramagnetic free energy is

$$F_P = 3\varepsilon_{Cu}n_{Cu} + 4E_{bandP}(n_{Fe}) + E_{FK} - 4T \ln(5) - 3T(S_{Cu} + S'_{Cu}). \quad (15)$$

From these equations, by minimization, we determine $n_{Cu}(T)$ and $m(T)$ corresponding to the lowest free energy. Hereafter we take $\varepsilon_{Fe} = 0$ and $t'^2 = 6t^2$.

3. Results and discussion

Let us first consider the behavior of the density of states in the F, P, and AF phases. In figure 2, we show the evolution of the ferromagnetic density of states $\rho_F(m, \omega)$ for spin \uparrow (ρ_{F+}) and \downarrow (ρ_{F-}) with the magnetization m . For spin up (down) the bandwidth is given by $9.8t\sqrt{v_+}$ ($9.8t\sqrt{v_-}$). For $m = 0$, this figure shows the paramagnetic density of states $\rho_P(\omega)$ and the bandwidth reduces to $6.93t$. For $m = 1$, we can see a wide band ($9.8t$) with a maximum kinetic energy and we have a ferromagnetic metal (FM). In figure 3, we show the antiferromagnetic density of states $\rho_{AF}(m, \omega)$. In this case, the density of states for spin σ , has two identical bands with bandwidth $4.9t\sqrt{v_-}$ separated by a gap given by $E_g^\sigma = 4.9t(\sqrt{v_+} - \sqrt{v_-})$. Besides these bands, for $\omega = 0$ and $m \neq 0$, the spectrum also shows δ -peaks arising from the poles of the Green's functions. For $m = 0$, $E_g^\sigma = 0$ and we recover the paramagnetic $\rho_P(\omega)$. When m is increased, the bands narrow and their spectral weight is diminished, therefore the gain in kinetic energy decreases. For $m = 1$, the kinetic energy reduces to zero and an antiferromagnetic insulator (AFI) phase occurs.

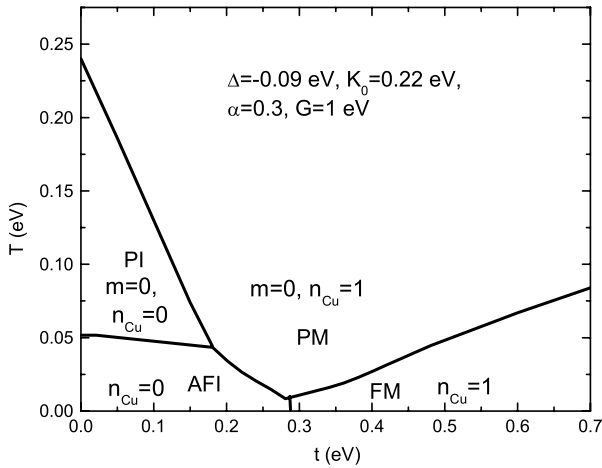


Figure 4. The temperature-hopping (pressure) phase diagram. The model shows four phases: antiferromagnetic metal (AFI), ferromagnetic metal (FM), paramagnetic insulator (PI), and paramagnetic metal (PM). At zero-temperature the figure shows a first-order transition from the AFI to FM at $t \simeq 0.28$ eV. Note that n_{Cu} changes from 0 to 1. For $t < 0.18$ eV, at low temperatures the model gives an AFI-PI transition and at high temperatures the PI-PM transition takes place. For $0.18 \text{ eV} < t < 0.28 \text{ eV}$, we have the transition from AFI to PM. For $t > 0.28 \text{ eV}$ we obtain only the transition from FM to PM with $n_{\text{Cu}} = 1$ in both phases. The parameters are adjusted taking into account the experimental results from Long *et al.*

The free energy equations (13) and (14) depend on two variables, m and n_{Cu} , and five parameters, $\Delta = (\varepsilon_{\text{Fe}} - \varepsilon_{\text{Cu}})$, G , t , K_0 , and temperature (T). At $T = 0$, the minima correspond to $m = 1$ in both phases. Further, to obtain a first-order transfer of electrons from Fe to Cu, we have chosen G as the largest parameter of the model so that the repulsion between extended and local electrons dominates in the minimization of the energy, so that the minima fall into $n_{\text{Cu}} = 0$ or $n_{\text{Cu}} = 1$.

For $t \ll K_0$, the minimum free energy corresponds to $n_{\text{Cu}} = 0$ and the AFI is stable. From equation (13) we obtain $F_{\text{AF}} = -K_0$. In contrast, for $K_0 \ll t$, the minimum corresponds to $n_{\text{Cu}} = 1$ and the model minimum energy corresponds to the FM phase. Equation (14) reduces to $F_{\text{F}} = 3\varepsilon_{\text{Cu}} + 4E_{\text{bandF}} + K_0 + 3G/4$. Solving equations (9) and (10) we obtain $E_{\text{bandF}} = E_{\text{bandF}}(m = 1, n_{\text{Fe}} = 1/4) = -0.796t$. Then, increasing the hopping parameter t , the model shows a phase transition from AFI to FM.

For $T \neq 0$, we adjust the model parameters to obtain the extrapolated Néel temperature and the transition temperature according to Long *et al.*'s experimental results in a suitable bandwidth. For this purpose, we take (the more difficult parameter to estimate) $G = 1 \text{ eV}$, $\Delta = -0.09 \text{ eV}$, $K_0 = 0.22 \text{ eV}$, and we fix the constant $\alpha = 0.3$. With this choice of parameters we show that the AFI phase jumps into an FM phase at $T = 0$ for $t \simeq 0.28 \text{ eV}$.

If we take any other reasonable choice of these parameters, no different qualitative results are obtained.

Using these parameters we obtain the phase diagram, T versus t , shown in figure 4. We take the hopping parameter t as an independent variable that can be modified by pressure. For $t < 0.18 \text{ eV}$, the model gives a paramagnetic insulator

phase (PI) between the low temperature AFI phase and the high temperature PM. In the PI phase, the Cu levels are empty ($n_{\text{Cu}} = 0$) and the system increases only the magnetic entropy ($m = 0$) to lower the free energy. Therefore, we can see two phase transitions: by increasing temperature we can observe first a transition from AFI to PI, where n_{Cu} remains zero without charge transfer. At higher temperatures a second transition from PI to PM takes place with valence changes and without magnetic order. For $0.18 \text{ eV} < t < 0.28 \text{ eV}$, when T increases, we have only one transition from AFI to PM where the magnetization changes and the charge transfer occur simultaneously: from $m \neq 0, n_{\text{Cu}} = 0$ to $m = 0, n_{\text{Cu}} = 1$. We speculate that this is the physics, in simplified terms, that governs Long *et al.*'s charge transfer results. Finally, for large values of t ($t > 0.28 \text{ eV}$), where the ferromagnetic kinetic energy is larger than the antiferromagnetic, the ground state is a ferromagnetic metal. with increasing temperature, a magnetic transition from FM to PM without charge transfer ($n_{\text{Cu}} = 1$) takes place.

4. Conclusions

We have presented a simple thermodynamic model for the simultaneous charge/spin order transition in $\text{LaCu}_3\text{Fe}_4\text{O}_{12}$. The model presented here allows us to understand, in simple terms, the mechanism that governs the phase transition and also allows us to speculate on the effect of pressure on this material to build a T - p phase diagram. We conclude that:

- (i) the transition is a Falikov-Kimball transition, i.e. it is a consequence of the Coulomb repulsion between extended Fe bands and localized Cu sites;
- (ii) the entropy difference that drives the transition at a critical temperature is mainly due to the Fe spin;
- (iii) assuming that the Fe bandwidth increases with pressure, the model allows us to propose the T - p phase diagram shown in figure 4, where it can be seen that the transition temperature first decreases with pressure and then, after an AF to F transition occurs, increases again;
- (iv) using the model, it is possible to calculate different thermodynamic properties of the phases: magnetization, magnetic susceptibility, specific heat, latent heat, occupation of extended states, etc; finally, we would like to emphasize that it would be desirable to obtain experimental results under pressure.

Acknowledgment

This work was supported by the Consejo Nacional de Investigaciones Científicas y Técnicas (CONICET).

References

- [1] Goodenough J B 2004 *Rep. Prog. Phys.* **67** 1915
- [2] Salamon M B and Jaime M 2001 *Rev. Mod. Phys.* **73** 583
- [3] Imada M, Fujimori A and Tokura Y 1998 *Rev. Mod. Phys.* **70** 1039
- [4] Lee P A, Nagaosa L and Wen X G 2006 *Rev. Mod. Phys.* **78** 17

- [5] Prinz G A 1998 *Science* **282** 1660
- [6] Coey J M D and Chien C L 2003 *MRS Bull.* **320** 720
- [7] Long Y W, Hayashi N, Saito T, Azuma M, Muranaka S and Shimakawa Y 2009 *Nature* **458** 60
- [8] Lee C, Kan E and Whangbo M-H 2009 arXiv:09044809
- [9] Falikov L M and Kimball J C 1969 *Phys. Rev. Lett.* **22** 997
Ramirez R, Falikov L M and Kimball J C 1970 *Phys. Rev. B* **2** 3383
- [10] Allub R and Alascio B 1997 *Phys. Rev. B* **55** 14113
- [11] Zener C 1951 *Phys. Rev.* **82** 403
- [12] Allub R, Navarro O, Avignon M and Alascio B 2002 *Physica B* **320** 13
- [13] Carvajal E, Navarro O, Allub R, Avignon M and Alascio B 2004 *J. Magn. Magn. Mater.* **272–276** 1774
- [14] Carvajal E, Navarro O, Allub R, Avignon M and Alascio B 2005 *Eur. Phys. J. B* **48** 179
- [15] See, e.g. Economou E N *Green's Functions in Quantum Physics* (*Springer Series in Solid States Sciences* vol 7) ed P Fulde (Berlin: Springer)